Inorganic Chemistry

Article

pubs.acs.org/IC

$SrGe_2B_2O_8$ and $Sr_3Ge_2B_6O_{16}$: Novel Strontium Borogermanates with Three-Dimensional and Layered Anionic Architectures

Yu-Cheng Hao,[†,‡] Chun-Li Hu,[†] Xiang Xu,[†] Fang Kong,[†] and Jiang-Gao Mao*[,†]

[†]State Key Laboratory of Structural Chemistry, Fujian Institute of Research on the Structure of Matter, Chinese Academy of Sciences, 155 Yangqiao Road West, Fuzhou 350002, P. R. China

[‡]University of Chinese Academy of Sciences, Beijing 100039, P. R. China

Supporting Information

ABSTRACT: Two new alkaline-earth strontium borogermanates, namely, $SrGe_2B_2O_8$ and $Sr_3Ge_2B_6O_{16}$, have been successfully synthesized through high-temperature solid state reactions. They represent the first examples of strontium borogermanates. $SrGe_2B_2O_8$ crystallized in space group *Pnma*, and its structure features a novel three-dimensional $[Ge_2B_2O_8]^{2-}$ framework composed of alternative linkages of the B_2O_7 and Ge_2O_7 dimeric units with one-dimensional (1D) tunnels of eight-membered rings (MRs) along the *b* axis that are filled by the Sr^{2+} cations. $Sr_3Ge_2B_6O_{16}$ is isostructural with $Ba_3Ge_2B_6O_{16}$ and crystallizes in centrosymmetric space group $P\bar{1}$. Its structure features a two-dimensional layer that is composed of circular B_6O_{16} clusters and GeO_4 tetrahedra that are interconnected via corner sharing, forming 1D four- and six-MR tunnels along *a* axis. Sr(1) cations are located in the six-MR tunnels, whereas Sr(2) cations are located in the interlayer space. Studies of their optical properties and thermal stability as well as band structure calculations based on density functional theory methods have been also performed.

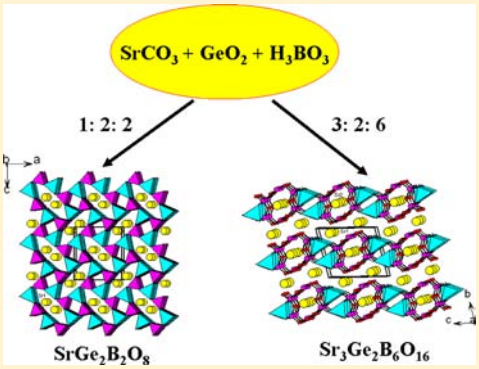

INTRODUCTION

Metal borates make up an important class of compounds for applications as nonlinear optical materials.[1] Recently, the family of metal borates has grown, and many boro-halides, boro-beryllates, aluminoborates, borosilicates, and boro-phosphates with abundant structures and good optical properties have been reported.[2−6] Naturally, the combination of borate and germanate groups gave birth of a new class of compounds, borogemanates. Various organically templated borogemanates with layered or three-dimensional (3D) network structures have been reported mainly by the groups of Zou and Yang.[7] It has been found that the size, shape, and charge of the template cations may direct the formation of a variety of open frameworks. A series of alkali metal borogermanates have been synthesized, among which $K_2GeB_4O_9{\cdot}2H_2O$, $AGeB_3O_7$ (A = Rb or Cs), $Rb_4Ge_3B_6O_{17}$, and $A_2GeB_4O_9$ (A = Rb or Cs) display moderately strong second-order nonlinear optical effects.[8] It has been found that reaction conditions such as the Ge/B ratio, reaction temperature, and size of the cation can have a strong effect on the chemical composition and crystal structures of the alkali metal borogermanates formed. For example, $RbGeB_3O_7$, $Rb_4Ge_3B_6O_{17}$, and $Rb_2GeB_4O_9$ have B/Ge molar ratio of 3/1, 2/1, and 4/1, respectively, and display three different 3D structures, though $A_2GeB_4O_9$ (A = Rb or Cs) species have a similar chemical composition, yet they crystallized in different space groups and display slightly different 3D network structures. A few transition metal borogermanates and lanthanide(III) borogermanates have been synthesized by hydrothermal or solid state reactions.[9] The alkaline-earth metal borogermanates have been explored less, and only three compounds, namely, $Ba_3Ge_2B_6O_{16}$, $Ba_3[Ge_2B_7O_{16}(OH)_2](OH)(H_2O)$, and $Ca_{10}Ge_{16}B_6O_{51}$, have been reported by our group.[10] The structure of germanium-rich $Ca_{10}Ge_{16}B_6O_{51}$ features a 3D B−Ge−O network composed of $[Ge_4O_{10.75}]_n$ layers that are further bridged by the BO_4 tetrahedra and B_2O_7 dimers, forming the one-dimensional (1D) tunnels of five-, six-, and seven-membered rings (MRs) along the *c* axis that are occupied by the Ca^{2+} ions. The polar $Ba_3[Ge_2B_7O_{16}(OH)_2](OH)(H_2O)$ features a novel 3D anionic framework composed of $[B_7O_{16}(OH)_2]^{13-}$ polyanions that are bridged by Ge atoms with 1D 10-MR tunnels along the *b* axis, whereas the centrosymmetric $Ba_3Ge_2B_6O_{16}$ exhibits a thick layer composed of circular B_6O_{16} cluster units interconnected by GeO_4 tetrahedra via corner sharing, forming 1D four- and six-MR tunnels along the *c* axis. It is known that the ionic radius of strontium(II) is between those of the calcium(II) and barium(II); hence, it is worth determining the structural similarities and differences between these alkaline-earth metal borogermanates. Therefore, we started a research program to explore new compounds in the $SrO−GeO_2−B_2O_3$ system. Two novel strontium borogermanates, namely, $SrGe_2B_2O_8$ and $Sr_3Ge_2B_6O_{16}$, have been synthesized and structurally characterized. Herein, we report their syntheses, crystal structures,

Received: August 29, 2013
Published: November 14, 2013

   dx.doi.org/10.1021/ic402214p | *Inorg. Chem.* 2013, 52, 13644−13650

optical and thermal behaviors, and electronic band structure calculations.

EXPERIMENTAL SECTION

Materials and Methods. H_3BO_3 (Shanghai Reagent Factory, 99.9%), GeO_2 (Shanghai Reagent Factory, 99.99%), and $SrCO_3$ (Alfa Aesar, 99.0%) were used without further purification. IR spectra were recorded on a Magna 750 FT-IR spectrometer as KBr pellets in the range of 4000−400 cm^{-1}. Microprobe elemental analyses of elements Sr and Ge were performed on a field-emission scanning electron microscope (JSM6700F) equipped with an energy-dispersive X-ray spectroscope (Oxford INCA). Powder X-ray diffraction (XRD) patterns were collected on a XPERT-MPD $\theta - 2\theta$ diffractometer using graphite-monochromated Cu Kα radiation in the 2θ range of 5−85° with a step size of 0.05°. Optical diffuse-reflectance spectra were recorded at room temperature with a PE Lambda 900 UV−visible spectrophotometer. The $BaSO_4$ plate was used as a standard (100% reflectance). The absorption spectrum was calculated from the reflectance spectrum using the Kubelka−Munk function $\alpha/S = (1 - R)^2/2R$,[11] where α is the absorption coefficient, S is the scattering coefficient, which is practically wavelength-independent when the particle size is >5 μm, and R is the reflectance. Thermogravimetric analysis (TGA) and differential scanning calorimetry (DSC) were conducted with a NETZSCH STA 449C unit at a heating rate of 15 °C/min under an oxygen atmosphere.

Syntheses of $SrGe_2B_2O_8$ and $Sr_3Ge_2B_6O_{16}$. Both compounds were synthesized by solid state reactions at high temperatures. The loaded compositions are $SrCO_3$ (0.2953 g, 2 mmol), GeO_2 (0.4144 g, 4 mmol), and H_3BO_3 (0.2473 g, 4 mmol) for $SrGe_2B_2O_8$, and $SrCO_3$ (0.4429 g, 3 mmol), GeO_2 (0.2092 g, 2 mmol), and H_3BO_3 (0.3710 g, 6 mmol) for $Sr_3Ge_2B_6O_{16}$. The reaction mixtures were thoroughly ground in an agate mortar and then transferred to a platinum crucible. The samples were heated at 900 °C for 3 days and then cooled to 400 °C at a cooling rate of 0.03 °C/min before the furnace was switched off. EDS elemental analyses of several single crystals of both compounds gave average Sr/Ge molar ratios of 1.0/2.1 and 3.0/2.1 for $SrGe_2B_2O_8$ and $Sr_3Ge_2B_6O_{16}$, respectively, which are in good agreement with those obtained from single-crystal X-ray diffraction studies (Figure S1 of the Supporting Information). After proper crystal structure determinations, colorless crystalline samples of $SrGe_2B_2O_8$ and $Sr_3Ge_2B_6O_{16}$ were obtained quantitatively by the reaction of a mixture of $SrCO_3$ (0.1476 g, 1 mmol), GeO_2 (0.2090 g, 2 mmol), and H_3BO_3 (0.1237 g, 2 mmol) (for $SrGe_2B_2O_8$) or $SrCO_3$ (0.4426 g, 3 mmol), GeO_2 (0.2093 g, 2 mmol), and H_3BO_3 (0.3713 g, 6 mmol) in a molar ratio of 3/2/6 (for $Sr_3Ge_2B_6O_{16}$) at 900 °C for 3 days. Their purities were confirmed by powder XRD studies (Figure S1 of the Supporting Information). IR data (KBr) for $SrGe_2B_2O_8$: 1102(s), 1050(s), 930(s), 847(s), 809(s), 643(m), 606(m), 582(m), 468(m), 430(w) cm^{-1}. IR data (KBr) for $Sr_3Ge_2B_6O_{16}$: 1369(s), 1264(m), 1106(s), 1074(s), 1023(s), 931(s), 765(m), 672(m), 622(m), 598(m), 525(w), 484(w) cm^{-1}.

Ion-Exchange Experiments. Ion-exchange reactions were performed with polycrystalline $SrGe_2B_2O_8$ (100 mg) and $Sr_3Ge_2B_6O_{16}$ (100 mg) in 2 mL of 0.3 mol/mL $BaCl_2$, $CdCl_2$, $HgCl_2$, and $PbCl_2$ solutions (all aqueous). Reactions were performed at room temperature for 24 h and then mixtures heated to 80 °C for 72 h. The ion-exchanged products were recovered by filtration, washed with excess water, and dried in air for 1 day.

Single-Crystal Structure Determination. Data for both compounds were collected on a SuperNova (Mo) X-ray source with Mo Kα radiation (λ = 0.71073 Å) at 293(2) K. Both data sets were corrected for Lorentz and polarization factors as well as for absorption by the multiscan method.[12a] Both structures were determined by direct methods and refined by a full-matrix least-squares fitting on F^2 by SHELX-97.[12b] Both structures were checked for possible missing symmetry elements using PLATON.[12c] Crystallographic data and structural refinements for both compounds are summarized in Table 1, and important bond distances are listed in Table 2. More information about the crystallographic studies and atomic displacement parameters are provided as Supporting Information.

Table 1. Crystal Data and Structural Refinements for $SrGe_2B_2O_8$ and $Sr_3Ge_2B_6O_{16}$

	$SrGe_2B_2O_8$	$Sr_3Ge_2B_6O_{16}$
formula weight	382.42	728.924
space group	*Pnma*	$P\bar{1}$
a (Å)	8.2622(5)	4.9978(5)
b (Å)	8.1084(4)	7.3292(7)
c (Å)	9.1513(5)	8.4576(8)
α (deg)	90.0	76.519(8)
β (deg)	90.0	77.282(8)
γ (deg)	90.0	89.575(8)
V (Å^3)	613.08(10)	293.56(10)
Z	4	1
D_c (g cm^{-3})	4.413	4.123
μ(Mo Kα) (mm^{-1})	18.421	18.708
GOF on F^2	0.940	1.066
R1, wR2 [$I > 2\sigma(I)$][a]	0.0234, 0.0556	0.0358, 0.0730
R1, wR2 (all data)[a]	0.0270, 0.0584	0.0448, 0.0781

[a] $R1 = \sum||F_o| - |F_c||/\sum|F_o|$, and $wR2 = [\sum w(F_o^2 - F_c^2)^2/\sum w(F_o^2)^2]^{1/2}$.

Computational Descriptions. Single-crystal structural data of both compounds were used for their electronic and optical property calculations. Band structures and densities of states (DOS) were determined with the total energy code CASTEP.[13] The total energy is calculated with density functional theory (DFT) using the Perdew−Burke−Ernzerhof generalized gradient approximation (GGA).[14] The interactions between the ionic cores and the electrons are described by the norm-conserving pseudopotential.[15] The following orbital electrons are treated as valence electrons: Sr $4p^6 5s^2$, Ge $4s^2 4p^2$, B $2s^2 2p^1$, and O $2s^2 2p^4$. The number of plane waves included in the basis set is determined by a cutoff energy of 750 eV, and the numerical integration of the Brillouin zone is performed using a 3 × 3 × 3 and 5 × 4 × 3 Monkhorst-Pack *k*-point sampling for $SrGe_2B_2O_8$ and $Sr_3Ge_2B_6O_{16}$, respectively. The other calculating parameters and convergent criteria were the default values of the CASTEP code.

Calculations of linear optical properties in terms of the complex dielectric function $\varepsilon(\omega) = \varepsilon_1(\omega) + i\varepsilon_2(\omega)$ were made. The imaginary part of the dielectric function ε_2 was given in the following equation[16]

$$\varepsilon_2^{ij}(\omega) = \frac{8\pi^2\hbar^2e^2}{m^2V}\sum_k\sum_{cv}(f_c - f_v)\frac{p_{cv}^i(k)p_{vc}^j(k)}{E_{vc}^2}$$
$$\delta[E_c(k) - E_v(k) - \hbar\omega]$$

where f_c and f_v represent the Fermi distribution functions of the conduction and valence bands, respectively. The term $p_{cv}^i(k)$ denotes the momentum matrix element transition from energy level *c* of the conduction band to level *v* of the valence band at a certain *k* point in the Brillouin zones, and *V* is the volume of the unit cell. *m*, *e*, and $\hbar$ are the electron mass, charge, and Plank's constant, respectively.

RESULTS AND DISCUSSION

Explorations of new phases in the Sr−Ge−B−O system led to the discovery of two new alkaline-earth borogermanates, namely, $SrGe_2B_2O_8$ and $Sr_3Ge_2B_6O_{16}$. They represent the first examples of strontium borogermanates. It is interesting to note that $SrGe_2B_2O_8$ and $Sr_3Ge_2B_6O_{16}$ were synthesized at different $SrCO_3/GeO_2/H_3BO_3$ molar ratios at the same reaction temperature; hence, the $SrCO_3/GeO_2/H_3BO_3$ molar ratio used in the reaction has a strong effect on the chemical composition and crystal structure of the resultant product.

dx.doi.org/10.1021/ic402214p | Inorg. Chem. 2013, 52, 13644−13650

Table 2. Important Bond Lengths (angstroms) for $SrGe_2B_2O_8$ and $Sr_3Ge_2B_6O_{16}$[a]

$SrGe_2B_2O_8$			
Ge−O(4)	1.733(2)	Ge−O(2)	1.731(2)
Ge−O(1)	1.7395(3)	Ge−O(3)	1.746(2)
B(1)−O	1.448(3)	B(1)−O(2)#1	1.457(4)
B(1)−O#2	1.448(3)	B(1)−O(3)#3	1.517(4)
B(1)−O(4)	1.494(4)	B(1)−O(3)#4	1.517(4)
Sr(2)−O(2)	2.602(2)	Sr(2)−O(4)	2.604(2)
Sr(2)−O(3)	2.587(2)	Sr(2)−O(3)#5	2.587(2)
Sr(2)−O(4)#6	2.604(2)	Sr(2)−O(2)#7	2.602(2)
Sr(2)−O(3)#8	3.043(2)	Sr(2)−O#9	2.516(3)
$Sr_3Ge_2B_6O_{16}$			
Ge−O(6)	1.726(4)	Ge−O(7)	1.732(4)
Ge−O(4)	1.741(4)	Ge−O(3)	1.745(4)
B(3)−O(9)#1	1.497(7)	B(1)−O(2)#2	1.497(7)
B(3)−O(6)#3	1.491(8)	B(2)−O(8)#4	1.328(8)
B(2)−O(2)#5	1.389(8)	B(1)−O(5)#6	1.445(7)
B(1)−O(3)	1.501(8)	B(3)−O(5)#7	1.460(7)
B(1)−O(7)#8	1.476(8)	B(3)−O(4)	1.475(8)
B(2)−O(9)	1.415(8)		
Sr(1)−O(8)	2.525(4)	Sr(1)−O(8)#9	2.560(4)
Sr(1)−O(6)	2.577(4)	Sr(1)−O(4)#10	2.594(4)
Sr(1)−O(7)#11	2.618(4)	Sr(1)−O(9)#12	2.703(4)
Sr(1)−O(3)	2.786(4)	Sr(1)−O(2)	2.766(4)
Sr(1)−O(9)#13	3.076(4)	Sr(2)−O(8)	2.508(4)
Sr(2)−O(8)	2.508(4)	Sr(2)−O(5)	2.614(4)
Sr(2)−O(2)	2.707(4)	Sr(2)−O(3)	2.794(4)
Sr(1)−O(9)#14	2.703(4)		

[a]Symmetry transformations used to generate equivalent atoms. For $SrGe_2B_2O_8$: #1, $-x+2, -y, -z+1$; #2, $x, -y+{}^1/_2, z$; #3, $-x+{}^3/_2, -y, z+{}^1/_2$; #4, $-x+{}^3/_2, -y, z-{}^1/_2$; #5, $x+{}^1/_2, y, -z+{}^3/_2$; #6, $-x+2, y+{}^1/_2, -z+1$; #7, $-x+{}^5/_2, -y, z-{}^1/_2$; #8, $-x+{}^5/_2, y+{}^1/_2, z-{}^1/_2$. For $Sr_3Ge_2B_6O_{16}$: #1, $x, y+1, z$; #2, $x, y-1, z$; #3, $x-1, y, z$; #4, $-x, -y+1, -z+1$; #5, $-x+1, -y+1, -z+1$; #6, $-x+1, -y, -z+1$; #7, $-x+1, -y-1, -z$; #8, $-x, -y+1, -z+1$; #9, $-x, -y, -z+1$; #10, $-x+1, -y, -z$; #11, $-x, -y, -z$; #12, $x-1, y-1, z$; #13, $x, y-1, z$; #14, $x+1, y+1, z$.

$SrGe_2B_2O_8$ belongs to a new structure type and crystallizes in centrosymmetric space group *Pnma*. Its structure features a unique 3D anionic framework composed of corner-sharing $[B_2O_7]$ and $[Ge_2O_7]$ dimers, forming 1D tunnels of eight-MRs that are filled by Sr^{2+} cations and four-MRs along the *b* axis. The symmetric unit of $SrGe_2B_2O_8$ contains one Sr atom on a mirror plane and one Ge atom and one B atom at the general sites. Both Ge and B atoms are tetrahedrally coordinated by four O atoms. The Ge−O and B−O distances are in the range of 1.731(2)−1.746(2) and 1.448(3)−1.517(4) Å, respectively, and O−Ge−O and O−B−O bond angles are in the range of 102.09(10)−113.79(13)° and 100.1(2)−114.5(3)°, respectively. These bond distances and angles are comparable to those reported in other borogermanates.[7−10] The Sr^{2+} cation is eight-coordinated by eight oxygen atoms with Sr−O bond distances in the range of 2.516(3)−2.604(2) Å. Bond valence calculations of the B and Ge atoms are in oxidation states of +3 and +4, respectively; the calculated total bond valences for B(1) and Ge(1) are +2.996 and +4.117, respectively, whereas those for O(1)−O(5) are −1.973, −2.088, −1.958, −2.070, and −1.986, respectively.[17]

A pair of BO_4 tetrahedra share corners in a B_2O_7 unit, as do a pair of GeO_4 tetrahedra (Figure 1a,b). These B_2O_7 and Ge_2O_7 units are further interconnected via corner sharing into a 3D $[Ge_2B_2O_8]^{2-}$ network with two types of 1D large tunnels along the *b* axis (Figure 1c). Each B_2O_7 unit connects with six Ge_2O_7 units and vice versa. The small vacant tunnels are based on four-MRs composed of two GeO_4 and two BO_4 tetrahedra, whereas the larger long and narrow tunnels filled by Sr^{2+} cations are based on eight-MRs composed of four GeO_4 and four BO_4 tetrahedra (Figure 1d).

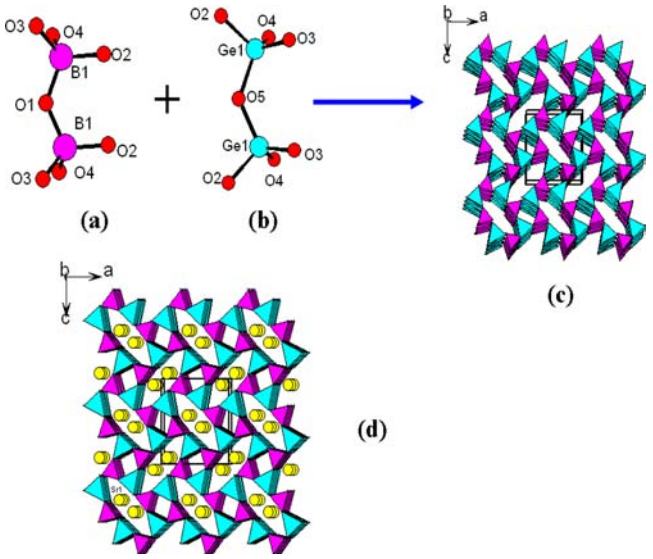

Figure 1. (a) B_2O_7 unit, (b) Ge_2O_7 unit, (c) view of the 3D $[Ge_2B_2O_8]^{2-}$ network down the *b* axis, and (d) view of the structure of $SrGe_2B_2O_8$ down the *b* axis. The GeO_4 and BO_4 tetrahedra are colored cyan and pink, respectively. The Sr atoms are drawn as yellow circles.

It is worth comparing the structure of $SrGe_2B_2O_8$ with that of $LiGeBO_4$, which also has a Ge/B molar ratio of 1/1.[8h] $LiGeBO_4$ crystallizes in NCS space group $I\bar{4}$ (No. 82), and its 3D framework consists of corner-linked BO_4 and GeO_4 tetrahedra that are in strict alternation, forming uniform 1D six-MR tunnels along the *c* axis that are occupied by Li^+ cations. The Li^+ ion is four-coordinated with four identical Li−O bonds of 1.994(1) Å. Hence, the dimerization of BO_4 and GeO_4 creates larger eight-MR tunnels that can accommodate the lager Sr^{2+} cations and smaller four-MR tunnels that are vacant. Hence, both the size and the charge of the cation exert strong effects on the structures of the compounds formed. Neighboring acentric BO_4 groups in $LiGeBO_4$ are aligned to produce an acentric structure.[3a] To accommodate the larger Sr^{2+} ions, both BO_4 and GeO_4 groups are dimerized. The two borate groups within the B_2O_7 dimer are related by a mirror plane, and these B_2O_7 dimers that have a very small net polarization are packed in antiparallel fashion because of the centrosymemtric space group adopted. Hence, the cation size also has a strong influence on the centricities of the materials.[18] It is interesting to note that $SrBPO_5$ has a 1D $[BPO_5]^{2-}$ anionic chain in which the 1D chain of corner-sharing BO_4 is further decorated by PO_4 tetrahedra, two vertices of the PO_4 tetrahedra remain terminal,[6a] and hence the anionic structure of $SrBPO_5$ has a dimension much lower than those of $SrGe_2B_2O_8$ and $LiGeBO_4$.

$Sr_3Ge_2B_6O_{16}$ is isostructural with $Ba_3Ge_2B_6O_{16}$, and its structure features a novel thick $[Ge_2B_6O_{16}]^{6-}$ anionic layer composed of cyclic B_6O_{16} units that are bridged by Ge atoms (Figure 2).[10a] The asymmetric unit of $Sr_3Ge_2B_6O_{16}$ contains two Sr atoms (one on an inversion center and one at a general site), one Ge atom, and three B atoms at general sites. The Ge

dx.doi.org/10.1021/ic402214p | *Inorg. Chem.* 2013, 52, 13644−13650

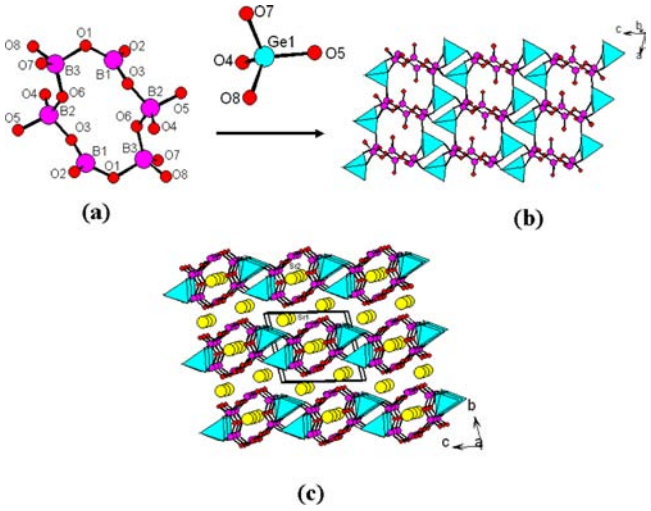

Figure 2. (a) B_6O_{16} cluster unit, (b) two-dimensional $[Ge_2B_6O_{16}]^{6-}$ layer in the $a-c$ plane, and (c) view of the structure of $Sr_3Ge_2B_6O_{16}$ down the a axis. The GeO_4 and BO_4 tetrahedra are colored cyan and pink, respectively. The Sr atoms are drawn as yellow circles.

atom is tetrahedrally coordinated by four O atoms with Ge−O distances falling in the range of 1.726(4)−1.745(4) Å and O−Ge−O bond angles in the range of 105.23(18)−114.84(19)°. Both B(1) and B(3) atoms are tetrahedrally coordinated, whereas the B(2) atom is in a triangular coordination geometry. The B−O bond distances of BO_3 tetrahedra [1.328(8)−1.415(8) Å] are significantly shorter than those of BO_4 tetrahedra [1.460(7)−1.497(7) Å]. The O−B−O angles for BO_3 and BO_4 groups are in the range of 115.5(6)−123.5(6)° and 103.1(5)−113.2(5)°, respectively. These bond distances and angles are comparable to those in $Ba_3Ge_2B_6O_{16}$ and other borogermanates reported previously.[7−10]

$B(2)O_4$ and $B(3)O_4$ groups are corner-sharing in a B_2O_7 unit, and two such B_2O_7 units are further bridged by two $B(1)O_3$ triangles in cycle B_6O_{16} clusters (Figure 2a). These B_6O_{16} units are further bridged by GeO_4 tetrahedra via corner-sharing into a two-dimensional (2D) $[Ge_2B_6O_{16}]^{6-}$ anionic layer parallel to the $a-c$ plane (Figure 2b). Within the $[Ge_2B_6O_{16}]^{6-}$ anionic layer, there are 1D tunnels of six-MRs along the a axis. The size of the tunnel is estimated to be 3.4 Å × 4.5 Å, which is large enough to accommodate the eight-coordinated Sr(2) atoms. The interlayer free space has a width of ∼3.1 Å, which is slightly shorter than that in $Ba_3Ge_2B_6O_{16}$ (3.47 Å). The eight-coordinated Sr(1) atoms are located in the interlayer space. The Sr−O distances are in the range of 2.508(4)−3.291(6) Å, which are slightly shorter than the Ba−O distances in $Ba_3Ge_2B_6O_{16}$. Bond valence calculations suggest that the B and Ge atoms are in oxidation states of +3 and +4, respectively, the calculated total bond valences for B(1), B(2), B(3), and Ge(1) atoms are 3.05, 3.00, 2.96, and 4.132, respectively, and those for O(1)−O(8) are −1.973, −1.985, −2.032, −1.998, −2.034, −1.975, −1.987, −2.103, and −2.057, respectively.[17]

Attempts to exchange Sr^{2+} with Ba^{2+}, Cd^{2+}, Hg^{2+}, and Pb^{2+} with similar ionic radii and the same valence with each other were tried; it was found that only Cd^{2+} can exchange with Sr^{2+}. For the Cd^{2+}-exchanged $SrGe_2B_2O_8$, the average Cd/Sr molar ratio is ∼1/4, the ion-exchange rate is ∼21%, and the resultant compound has a chemical composition close to $Sr_{0.79}Cd_{0.21}Ge_2B_2O_8$. For the Cd^{2+}-exchanged $Sr_3Ge_2B_6O_{16}$, the average Cd/Sr molar ratio is ∼1/2, the ion-exchange rate is ∼33%, and the ion-exchanged species has a chemical composition close to $Sr_2CdGe_2B_6O_{16}$ (Figure S2 of the Supporting Information).

TGA and DSC Studies. TGA studies indicate that both compounds display no obvious weight loss before 1100 °C (Figure 3). From the DSC function curves, $SrGe_2B_2O_8$ and

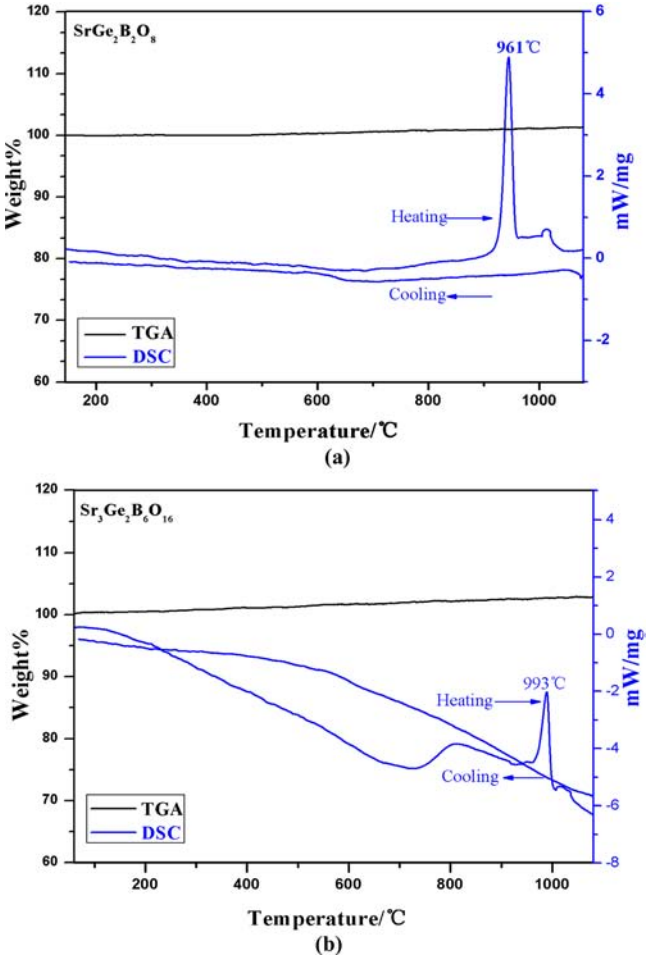

Figure 3. TGA and DSC curves for (a) $SrGe_2B_2O_8$ and (b) $Sr_3Ge_2B_6O_{16}$.

$Sr_3Ge_2B_6O_{16}$ exhibit endothermic peaks at 961 and 993 °C, respectively (Figure 3), which correspond to the melting points of the compounds. From the DSC curves, they have only endothermic peaks in the heating curves and no exothermic peaks in the cooling curves; hence, both compounds melt incongruently. To verify this point, we calcinated powder samples of $SrGe_2B_2O_8$ and $Sr_3Ge_2B_6O_{16}$ at 1000 °C for 10 h. The measured XRD powder patterns for the calcinated samples are different from those of the unheated samples; hence, $SrGe_2B_2O_8$ and $Sr_3Ge_2B_6O_{16}$ melt incongruently. After calcination, both $SrGe_2B_2O_8$ and $Sr_3Ge_2B_6O_{16}$ became amorphous and the residuals were not characterized further (Figure S1 of the Supporting Information).

Optical Properties. The optical diffuse reflectance spectra reveal that both $SrGe_2B_2O_8$ and $Sr_3Ge_2B_6O_{16}$ are insulators with optical band gaps of 5.31 and 5.83 eV, respectively (Figure S3 of the Supporting Information). The band gap of $Sr_3Ge_2B_6O_{16}$ is slightly larger than that of $Ba_3Ge_2B_6O_{16}$ (5.12 eV). The UV−vis−NIR absorption spectra of $SrGe_2B_2O_8$ and

dx.doi.org/10.1021/ic402214p | Inorg. Chem. 2013, 52, 13644−13650

$Sr_3Ge_2B_6O_{16}$ exhibit little absorption in the range of 300−2500 nm (Figure S4 of the Supporting Information), and their IR spectra show very high transmittance in the range of 4000−1600 cm^{-1} (2.50−6.25 μm) and 4000−1800 cm^{-1} (2.50−5.55 μm), respectively (Figure S5 of the Supporting Information). Hence, $SrGe_2B_2O_8$ and $Sr_3Ge_2B_6O_{16}$ are transparent in the range of 0.30−6.25 and 0.3−5.55 μm, respectively. The IR spectra of $Sr_3Ge_2B_6O_{16}$ display strong absorption bands at 1264−1369 cm^{-1} that can be assigned to the asymmetrical stretch of the BO_3 groups. For both $SrGe_2B_2O_8$ and $Sr_3Ge_2B_6O_{16}$, the bands associated with the BO_4 groups appeared in the range of 930−1106 cm^{-1}. The absorption peaks in the range of 765−847 cm^{-1} can be assigned to the asymmetrical stretch of the GeO_4 groups. The absorption bands in the range of 460−672 cm^{-1} correspond to the bending vibrations of the Ge−O bonds. The bending vibrations of BO_3 and BO_4 in $Sr_3Ge_2B_6O_{16}$ appeared in the range of 400−700 cm^{-1} (Figure S7 of the Supporting Information).[19] These assignments are consistent with those previously reported.[7−10]

Theoretical Studies. The calculated structures of $SrGe_2B_2O_8$ and $Sr_3Ge_2B_6O_{16}$ along high symmetry points of the first Brillouin zone are plotted in Figure S6 of the Supporting Information, and the state energies (electronvolts) of the lowest-conduction band (LCB) and the highest-valence band (HVB) of the two compounds are listed in Table 3. For

Table 3. State Energies (electronvolts) of the Lowest Conduction Band (L-CB) and the Highest Valence Band (H-VB) of the Crystals of $SrGe_2B_2O_8$ and $Sr_3Ge_2B_6O_{16}$

	k-point	L-CB	H-VB
$SrGe_2B_2O_8$	G(0.000 0.000 0.000)	4.32103	0
	Z(0.000 0.000 0.500)	4.99957	−0.02183
	T(−0.500 0.000 0.500)	5.29834	−0.06731
	Y(−0.500 0.000 0.000)	5.07632	−0.04763
	S(−0.500 0.500 0.000)	5.35248	−0.04712
	X(0.000 0.500 0.000)	5.19865	−0.07923
	U(0.000 0.500 0.500)	5.35489	−0.05373
	R(−0.500 0.500 0.500)	5.54596	−0.05546
$Sr_3Ge_2B_6O_{16}$	G(0.000 0.000 0.000)	4.98194	−0.05211
	F(0.000 0.500 0.000)	5.62202	−0.17864
	Q(0.000 0.500 0.500)	5.87151	−0.07805
	Z(0.000 0.000 0.500)	5.49804	0
	G(0.000 0.000 0.000)	4.98194	−0.05211

$SrGe_2B_2O_8$, both the lowest point of LCB (4.32 eV) and the highest point of HVB (0.0 eV) are at G point; therefore, it is a direct band gap insulator. For $Sr_3Ge_2B_6O_{16}$, the lowest point of LCB (4.98 eV) is localized at G point and the highest point of H-VB (0.0 eV) is at Z point; therefore, it is an indirect band gap insulator. The calculated band gaps (4.32 and 4.98 eV) are smaller than experimental values (5.31 eV for $SrGe_2B_2O_8$ and 5.84 eV for $Sr_3Ge_2B_6O_{16}$). This is not surprising because it is well-known that the DFT-GGA does not accurately describe the eigenvalues of the electronic states, causing the quantitative underestimation of band gaps, especially for insulators.[20] Hence, in the subsequent calculations of the linear optical properties, scissors of 0.99 and 0.86 eV are adopted for $SrGe_2B_2O_8$ and $Sr_3Ge_2B_6O_{16}$, respectively.

The bands can be assigned according to the total and partial DOS (Figure S7 of the Supporting Information). It is clear that their DOS curves are very similar to each other, so we take $SrGe_2B_2O_8$ as an example to analyze them in detail. For $SrGe_2B_2O_8$, the lowest VB around −31.0 eV is fully contributed by isolated Sr 5s states. The peaks in the range of −20.3 to −17.0 eV mainly arise from O 2s states, mixing with small amounts of B 2s2p and Ge 4s4p states. The peak localized around −14.4 eV is mostly contributed by isolated Sr 4p states. In the vicinity of the Fermi level, namely, −9.4 to 0 eV in the VB and 5.0−15.0 eV in the CB, B 2s2p, Ge 4s4p, and O 2p states are all involved and overlap fully among them, indicating the strong covalent interactions of Ge−O and B−O bonds in the system. Meanwhile, in the whole VB and CB region, B 2s and B 2p as well as Ge 4s and Ge 4p are overlapped in the same energy ranges, representing the obvious s-p hybridization of B and Ge atoms.

The results of population analyses (Table S1 of the Supporting Information) indicate that, for two compounds, the calculated bond orders of Ge−O and B−O bonds are 0.54−0.56 and 0.58−0.92 e (that of a standard covalent single bond is generally 1.0 e), respectively. In addition, the B−O bond orders of 0.74−0.92 e for the BO_3 groups are much larger than those of 0.59−0.72 e for the BO_4 groups. The bond orders of Sr−O bonds are very small (0.01−0.13 e) because they are mainly ionic in nature.

The linear optical response properties of the compounds were examined by calculating the complex dielectric function $\varepsilon(\omega) = \varepsilon_1(\omega) + i\varepsilon_2(\omega)$. Its imaginary part $[\varepsilon_2(\omega)]$ can be used to describe the real transitions between the occupied and unoccupied electronic states. The imaginary and real parts of the frequency-dependent dielectric functions show obvious anisotropy along three coordination directions (Figures S8 and S9 of the Supporting Information). The curves of the averaged imaginary parts and real parts of dielectric functions were obtained from the equation $\varepsilon^{ave} = (\varepsilon_x + \varepsilon_y + \varepsilon_z)/3$ (Figure 4).

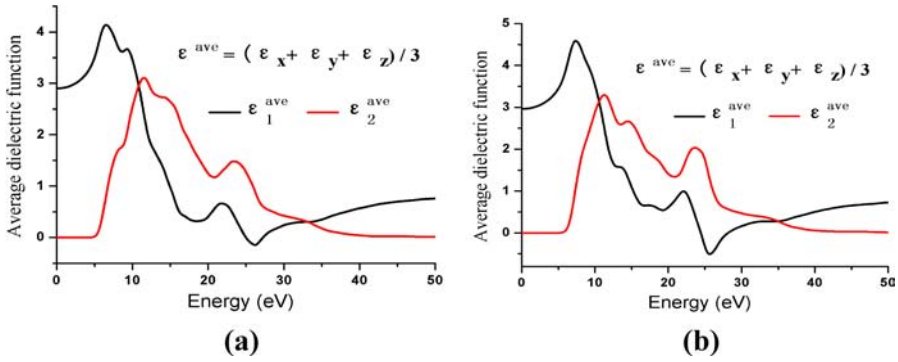

Figure 4. Calculated average imaginary part and real part of the dielectric function for (a) $SrGe_2B_2O_8$ and (b) $Sr_3Ge_2B_6O_{16}$.

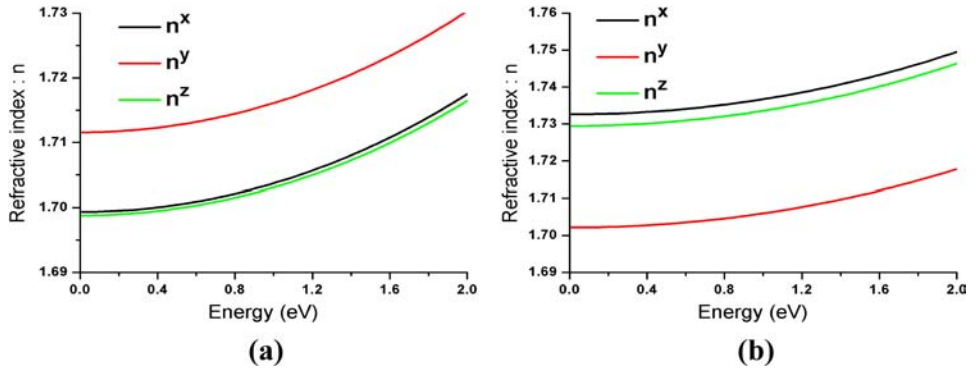

Figure 5. Calculated linear refractive indices for (a) $SrGe_2B_2O_8$ and (b) $Sr_3Ge_2B_6O_{16}$.

The averaged imaginary parts reveal the strongest adsorption peaks of $SrGe_2B_2O_8$ and $Sr_3Ge_2B_6O_{16}$ are at 11.6 and 11.2 eV, respectively, which can be mainly assigned to the electronic interband transitions from the O 2p to B 2p and Ge 4s states. The average static dielectric constant $\varepsilon(0)$ values of $SrGe_2B_2O_8$ and $Sr_3Ge_2B_6O_{16}$ are 2.90 and 2.96, respectively. The dispersion curves of refractive indices calculated by the formula $n^2(\omega) = \varepsilon(\omega)$ display obvious anisotropy that arises from the anisotropy of the dielectric functions, and the refractive indices decrease in the following order: $n^y > n^x > n^z$ for $SrGe_2B_2O_8$ and $n^x > n^z > n^y$ for $Sr_3Ge_2B_6O_{16}$ in the low-energy range (Figure 5). The static values of n^x, n^y, and n^z (at 0.0 eV) are calculated to be 1.699, 1.712, and 1.698 for $SrGe_2B_2O_8$ and 1.733, 1.702, and 1.729 for $Sr_3Ge_2B_6O_{16}$, respectively.

CONCLUSIONS

In summary, the first two examples of strontium borogermanates, namely, $SrGe_2B_2O_8$ and $Sr_3Ge_2B_6O_{16}$, have been prepared and structurally characterized. Interestingly, both of them are synthesized by high-temperature solid state reactions. They prove that more and more alkaline-earth borogermanates can be prepared with proper methods. $SrGe_2B_2O_8$ features a novel 3D anionic framework composed of Ge_2O_7 and B_2O_7 dimers that are interconnected alternatively via corner sharing. They form two kinds of tunnels, the large one being filled with two Sr^{2+} cations, whereas $Sr_3Ge_2B_6O_{16}$ exhibits a 2D layer structure based on B_6O_{16} units linked by GeO_4 tetrahedra. Both of them have relatively large tunnels, which allow them to be ion-exchanged by Cd^{2+} based on resultes from EDS. Our future research efforts will be focused on the explorations of borogermanates of other alkaline-earth metals and divalent metal ions such as Mg^{2+}, Zn^{2+}, Pb^{2+}, Hg^{2+}, etc.

ASSOCIATED CONTENT

Supporting Information

X-ray crystallographic files in CIF format, calculated bond orders, simulated and experimental powder XRD patterns, UV−IR spectra, optical diffuse reflectance, bond structures, DOS diagrams, and the imaginary and real parts of dielectric constant ε. This material is available free of charge via the Internet at http://pubs.acs.org.

AUTHOR INFORMATION

Corresponding Author

*E-mail: mjg@fjirsm.ac.cn. Fax: (+86)591-83714946.

Notes

The authors declare no competing financial interest.

ACKNOWLEDGMENTS

This work was supported by the National Natural Science Foundation of China (Grants 21231006, 21373222, and 21001107).

REFERENCES

(1) (a) Chen, C. T.; Wu, B. C.; Jiang, A. D.; You, G. M. *Sci. Sin., Ser. B (Engl. Ed.)* **1985**, *18*, 235. (b) Chen, C. T.; Liu, G. Z. *Annu. Rev. Mater. Sci.* **1986**, *16*, 203. (c) Chen, C. T.; Wu, Y. C.; Jiang, A. D.; Wu, B. C.; You, G. M.; Li, R. K.; Lin, S. J. *J. Opt. Soc. Am. B* **1989**, *6*, 616. (d) Becker, P. *Adv. Mater.* **1998**, *13*, 979. (e) Chen, C. T.; Wang, Y. B.; Wu, B. C.; Wu, K. C.; Zeng, W. L.; Yu, L. H. *Nature* **1995**, *373*, 322. (f) Zhang, W. L.; Cheng, W. D.; Zhang, H.; Geng, L.; Lin, C. S.; He, C. Z. *J. Am. Chem. Soc.* **2010**, *132*, 1508. (g) Kong, F.; Huang, S. P.; Sun, Z. M.; Mao, J. G.; Cheng, W. D. *J. Am. Chem. Soc.* **2006**, *128*, 7750. (h) Pan, S. L.; Smit, J. P.; Watkins, B.; Marvel, M. R.; Stern, C. L.; Poeppelmeier, K. R. *J. Am. Chem. Soc.* **2006**, *128*, 11631.

(2) (a) Huang, Y. Z.; Wu, L. M.; Wu, X. T.; Li, L. H.; Chen, L.; Zhang, Y. F. *J. Am. Chem. Soc.* **2010**, *132*, 12788. (b) Wu, H.; Yu, H.; Yang, Z.; Hou, X.; Su, X.; Pan, S.; Poeppelmeier, K. R.; Rondinelli, J. M. *J. Am. Chem. Soc.* **2013**, *135*, 4215. (c) Huang, H. W.; Yao, J. Y.; Lin, Z. S.; Wang, X. Y.; He, R.; Yao, W. J.; Zhai, N. X.; Chen, C. T. *Angew. Chem., Int. Ed.* **2001**, *50*, 9141. (d) Wu, H. P.; Pan, S. L.; Li, H. Y.; Jia, D. Z.; Chen, Z. H.; Fan, X. Y.; Yang, Y.; Rondinelli, J. M.; Luo, H. S. *J. Am. Chem. Soc.* **2011**, *133*, 7786.

(3) (a) Wang, S. C.; Ye, N.; Li, W.; Zhao, D. *J. Am. Chem. Soc.* **2010**, *132*, 8779. (b) Wang, S. C.; Ye, N. *J. Am. Chem. Soc.* **2011**, *133*, 11458. (c) Yan, X.; Luo, S. Y.; Lin, Z. S.; Yue, Y. C.; Wang, X. Y.; Liu, L. J.; Chen, C. T. *J. Mater. Chem. C* **2013**, *1*, 3616.

(4) (a) Yang, T.; Bartoszewicz, A.; Ju, J.; Sun, J. L.; Liu, Z.; Zou, X. D.; Wang, Y. X.; Li, G. B.; Liao, F. H.; Martin-Matute, B.; Lin, J. H. *Angew. Chem., Int. Ed.* **2011**, *50*, 12555. (b) Zhou, J.; Fang, W. H.; Rong, C.; Yang, G. Y. *Chem.—Eur. J.* **2010**, *16*, 4852. (c) Ju, J.; Yang, T.; Li, G. B.; Liao, F. H.; Wang, Y. X.; You, L. P.; Lin, J. H. *Chem.—Eur. J.* **2004**, *10*, 3901.

(5) Wu, H. P.; Yu, H. W.; Pan, S. L.; Huang, Z. J.; Yang, Z. H.; Su, X.; Poeppelmeier, K. R. *Angew. Chem., Int. Ed.* **2013**, *52*, 3406.

(6) (a) Pan, S. L.; Wu, Y. C.; Fu, P. Z.; Zhang, G. C.; Li, Z. H.; Du, C. X.; Chen, C. T. *Chem. Mater.* **2003**, *15*, 2218. (b) Sevov, S. C. *Angew. Chem., Int. Ed.* **1996**, *35*, 2630. (c) Lin, Z. H.; Wu, Y. C.; Fu, P. Z.; Wang, Z. Z.; Chen, C. T. *Chem. Mater.* **2004**, *16*, 2906.

(7) (a) Dadachov, M. S.; Sun, K.; Conradsson, T.; Zou, X. D. *Angew. Chem., Int. Ed.* **2000**, *39*, 3674. (b) Li, Y.; Zou, X. D. *Angew. Chem., Int. Ed.* **2005**, *44*, 2012. (c) Pan, C. Y.; Liu, G. Z.; Zheng, S. T.; Yang, G. Y. *Chem.—Eur. J.* **2008**, *14*, 5057. (d) Wang, G. M.; Sun, Y. Q.; Yang, G. Y. *Cryst. Growth Des.* **2005**, *5*, 313. (e) Zhang, H. X.; Zhang, J.; Zheng, S. T.; Yang, G. Y. *Inorg. Chem.* **2005**, *44*, 1166.

(8) (a) Lin, Z. E.; Zhang, J.; Yang, G. Y. *Inorg. Chem.* **2003**, *42*, 1797. (b) Zhang, H. X.; Zhang, J.; Zheng, S. T.; Wang, G. M.; Yang, G. Y. *Inorg. Chem.* **2004**, *43*, 6148. (c) Kong, F.; Jiang, H. L.; Hu, T.; Mao, J. G. *Inorg. Chem.* **2008**, *47*, 10611. (d) Xiong, D. B.; Zhao, J. T.; Chen,

H. H.; Yang, X. X. *Chem.—Eur. J.* **2007**, *13*, 9862. (e) Parise, J. B.; Gier, T. E. *Chem. Mater.* **1992**, *4*, 1065. (f) Zhang, J. H.; Hu, C. L.; Xu, X.; Kong, F.; Mao, J. G. *Inorg. Chem.* **2011**, *50*, 1973. (g) Xu, X.; Hu, C. L.; Kong, F.; Zhang, J. H.; Mao, J. G.; Sun, J. L. *Inorg. Chem.* **2013**, *52*, 5831. (h) Parise, J. B.; Gier, T. E. *Chem. Mater.* **1992**, *4*, 1065.

(9) (a) Zhang, J. H.; Li, P. X.; Mao, J. G. *Dalton Trans.* **2010**, *39*, 5301. (b) Zhang, J. H.; Kong, F.; Xu, X.; Mao, J. G. *J. Solid State Chem.* **2012**, *195*, 63 and references cited therein.

(10) (a) Zhang, J. H.; Kong, F.; Mao, J. G. *Inorg. Chem.* **2011**, *50*, 3037. (b) Xu, X.; Hu, C. L.; Kong, F.; Zhang, J. H.; Mao, J. G. *Inorg. Chem.* **2011**, *50*, 8861.

(11) Wendlandt, W. M.; Hecht, H. G. *Reflectance Spectroscopy*; Interscience: New York, 1966.

(12) (a) *CrystalClear*, version 1.3.5; Rigaku Corp.: The Woodlands, TX, 1999. (b) Sheldrick, G. M. *SHELXTL, Crystallographic Software Package*, version 5.1; Bruker-AXS: Madison, WI, 1998. (c) Spek, A. L. *PLATON*; Utrecht University: Utrecht, The Netherlands, 2001.

(13) (a) Segall, M. D.; Lindan, P. J. D.; Probert, M. J.; Pickard, C. J.; Hasnip, P. J.; Clark, S. J.; Payne, M. C. *J. Phys.: Condens. Matter* **2002**, *14*, 2717. (b) Milman, V.; Winkler, B.; White, J. A.; Pickard, C. J.; Payne, M. C.; Akhmatskaya, E. V.; Nobes, R. H. *Int. J. Quantum Chem.* **2000**, *77*, 895.

(14) Perdew, J. P.; Burke, K.; Ernzerhof, M. *Phys. Rev. Lett.* **1996**, *77*, 3865.

(15) Lin, J. S.; Qteish, A.; Payne, M. C.; Heine, V. *Phys. Rev. B* **1993**, *47*, 4174.

(16) Bassani, F.; Parravicini, G. P. *Electronic States and Optical Transitions in Solids*; Pergamon Press Ltd.: Oxford, U.K., 1975; p 149.

(17) (a) Brown, I. D.; Altermatt, D. *Acta Crystallogr.* **1985**, *B41*, 244. (b) Brese, N. E.; O'Keeffe, M. *Acta Crystallogr.* **1991**, *B47*, 192.

(18) Zou, G.; Ye, N.; Huang, L.; Lin, X. *J. Am. Chem. Soc.* **2011**, *133*, 20001.

(19) Nakamoto, K. *Infrared Spectra of Inorganic and Coordination Compounds*; Wiley: New York, 1970.

(20) (a) Godby, R. W.; Schluther, M.; Sham, L. *J. Phys. Rev. B* **1987**, *36*, 6497. (b) Okoye, C. M. I. *J. Phys.: Condens. Matter* **2003**, *15*, 5945. (c) Terki, R.; Bertrand, G.; Aourag, H. *Microelectron. Eng.* **2005**, *81*, 514. (d) Jiang, H. L.; Kong, F.; Mao, J. G. *J. Solid State Chem.* **2007**, *180*, 1764.